

O F



45
50
56
63
71
80
90
100



MICROCOPY RESOLUTION TEST CHART
NATIONAL BUREAU OF STANDARDS
STANDARD REFERENCE MATERIAL 1010a
(ANSI and ISO TEST CHART No. 2)

F. QUERCIA, M. D'ALESSANDRO, A. SALTELLI

PERFORMANCE ASSESSMENT OF AN ALPHA-WASTE DEPOSIT IN A CLAY-FORMATION

IT8800889



**COMITATO NAZIONALE PER LA RICERCA E PER LO SVILUPPO
DELL'ENERGIA NUCLEARE E DELLE ENERGIE ALTERNATIVE**

PERFORMANCE ASSESSMENT OF AN ALPHA-WASTE DEPOSIT IN A CLAY-FORMATION

F. QUERCIA

**ENEA - Direzione Sicurezza Nucleare e Protezione Sanitaria - Settore Ambiente Radioprotezione
Divisione Radioattività Ambientale, Sede Roma - EUR**

**M. D'ALESSANDRO, A. SALTELLI
CER-Joint Research Centre - Ispra**

Testo pervenuto nell'ottobre 1987
Progetto Enea: Attività di ricerca (HC)

I contenuti tecnico-scientifici dei rapporti tecnici dell'Enea
rispecchiano l'opinione degli autori e non necessariamente quella dell'ente.

SUMMARY

The probabilistic code LISA (Long term Isolation Safety Assessment) has been used to assess the risk related to the disposal of alpha waste in a geological formation.

The code has been modified to take into account waste form properties and leaching processes pertinent to alpha waste produced at fuel reprocessing plants.

The exercise refers to a repository in a deep clay formation located at Harwell (U.K.) where some hydrogeological data were available.

Radionuclide migration through repository and geological barriers has been simulated together with biosphere contamination.

Results of the assessment are presented as dose rate (or risk) distributions; a sensitivity analysis on input parameters has been performed.

RIASSUNTO

Allo scopo di valutare il rischio legato allo smaltimento di rifiuti radioattivi alfa in una formazione geologica è stato utilizzato il codice probabilistico LISA.

Tale codice, originariamente concepito per i rifiuti vetrificati ad alta attività, è stato modificato per tenere conto dei processi di degradazione e lisciviazione della matrice di condizionamento dei rifiuti alfa provenienti dagli impianti di riprocessamento del combustibile nucleare. La presente analisi si riferisce ad una formazione argillosa situata ad Harwell (U.K.) di cui erano disponibili i dati idrogeologici. Il modello adottato simula la migrazione dei radionuclidi attraverso le barriere del deposito e della formazione geologica e il trasferimento alla biosfera.

I risultati della valutazione sono presentati in forma di distribuzioni della dose annuale (o del rischio); è stata anche condotta una analisi di sensibilità sui parametri del modello.

CONTENT

1. INTRODUCTION	1
2. METHODOLOGY AND CODE	2
3. CONCEPTUAL SITE CHARACTERISTICS	4
3.1 Geohydrology of the site	4
3.2 Repository design	6
3.3 Waste inventory	6
4. RELEASE SCENARIO	7
4.1 Normal scenario	7
5. MODELLING	8
5.1 Concrete degradation and near-field diffusion	8
5.2 Far-field model	12
5.3 Biosphere	12
6. RESULTS	13
7. SENSITIVITY ANALYSIS	14
8. CONCLUSIONS	16

1. INTRODUCTION

In the framework of the exercise PAGIS (Performance Assessment of Geological Isolation System) /1/, a methodological approach was defined to analyse the risk linked to the disposal of vitrified high-level waste into deep geological formations /2/. It makes use of probabilistic criteria, and is in agreement with the guidelines suggested in a recent publication of the ICRP /3/.

In this context, the statistical code LISA (Monte Carlo type) has been developed at the JRC-Ispra; it calculates radiation exposures and risks associated with radionuclide releases from geological repositories of nuclear waste /4/. In a previous assessment the LISA code was applied to the analysis of a repository for high level vitrified waste in a clay-formation /5/. This study is intended to test the applicability of the above-mentioned methodology and computer code for different conditioning matrices and in different repository situations. This provides a preliminary basis for a future evaluation of the risk linked to the geological disposal of any type of long-lived waste.

The present work represents a pilot study only, and the results are of preliminary nature. A number of methodological and modelling aspects previously defined for the study of high-level waste repositories are common also to other waste types, in particular the probabilistic treatment, the migration/retention process modelling in geo- and bio-sphere, the radiological calculations and statistical analysis. There are, however, significant differences concerning waste inventory (quantities and radiological properties), conditioning matrices (physico-chemical properties, leaching behaviour) and repository design (size, structural materials, canister spatial distribution) which make that both source term and near-field modelling must be revised. Another difference is related to the larger degree of uncertainty which affects the whole assessment, as many of the input parameters and some models describing the leaching behaviour of various potential conditioning matrices have not yet been sufficiently investigated. As a consequence,

in this exercise emphasis is placed on conditioned waste leaching modelling and near-field description.

During a preparatory meeting held at Ispra with some experts of the EEC it was suggested that the geological formations considered for the present exercise should be chosen among those already listed for PAGIS; it was, therefore, decided to work out a hypothetical alpha-waste repository mined in the Oxford clay (UK), as clay formations appear especially suitable for non-heat-generating wastes. However it must be emphasized that the present assessment represents just an exercise aimed at checking the methodology and must not be interpreted as an evaluation of the suitability or safety of the site.

2. METHODOLOGY AND CODE LISA

The assessment methodology consists of a number of steps:

- 1) identification and description of the different scenarios involving radionuclide release from the repository;
- 2) assessment of the probabilities of occurrence of the various events capable of triggering or perturbing the release scenarios;
- 3) modelling of the radionuclide release and transport through the various system components, following the scenario considered; modelling of the radionuclide dispersion in the environment, assessment of their concentrations in food chains and related intake to man;
- 4) assessment of the radiation exposures to individuals, in terms of effective dose equivalent;
- 5) conversion of doses to risk;
- 6) investigation of the relative importance of the various input parameters in governing the output.

Points 1) and 2) require the identification of all the events and processes which could either initiate release of radionuclides from the waste, and cause their transport through the geosphere and the biosphere to man, or could influence their release and transport rates. For any

given type of geologic formation, there will be some processes which are certain to occur; they constitute the "normal evolution scenario". The assumptions used in analysing this scenario are based on extrapolations into the future of present geological and climatic trends. Probabilistic events and processes, having the capability to perturb the normal situation, lead to the definition of the "altered evolution scenarios", characterized by different parameter values. Among probabilistic scenarios, accidental and catastrophic events with very low probabilities, are sometimes considered.

Points 3) and 4) require that numerical values be assigned to the parameters used in the analysis. For parameters which cannot be univocally determined, either because of their intrinsic variability in space and time, or because of poor experimental knowledge, probability density functions are assigned to cover their entire range of variability. These distributions have, as a rule, a familiar form: uniform, normal or lognormal distributions are the most common. They are fed into the computer code, which uses them to generate the sets of values for the Monte Carlo simulations, and produces model outputs (e.g. annual doses) which are again in the form of probability distributions (histograms).

The output from LISA is a distribution of the risk. It is built, first, by generating a large number of dose rate curves as a function of time, each curve being associated with a particular set of input data, then, the peak doses are gathered into a histogram. This latter is finally transformed into a histogram of the risk, by multiplying each column by the risk factor (10^{-2} Sv^{-1}).

For probabilistic scenarios, whose probability of occurrence is small, the peak doses are also multiplied by the probability of the scenario itself; this product is taken to be the probability that individuals will receive exposures. Thus, a histogram of the risk linked to the given accidental scenario is generated.

This latter histogram can be further elaborated by summing up the areas of the columns, each one being weighted by its frequency φ_i :

$$R_T = \sum R_i \cdot \phi_i$$

where R_T is the total risk (1/a) associated with the given scenario. This figure of risk may then be compared with any pre-established risk limit.

Finally, (point 6) the statistical analysis of the results permits to investigate the relative importance of the various uncertain parameters thus pointing out those parameters and research areas which deserve further investigations.

3. CONCEPTUAL SITE CHARACTERISTICS

3.1 Geohydrology of the site

The conceptual site utilized for the present study is Harwell, where local data on groundwater regime and geohydrological properties of the sedimentary sequence are available. A detailed study of the groundwater regime of the area, on a regional and local scale, was recently carried out (/6 and 7/). The Oxford Clay at Harwell site lies 262 to 328 metres below ground surface (Fig. 1). This formation appears as a silty mudstone that is often fissile and calcareous. Calcitic bivalve and coalified plant-debris are also common. Oxford clay appears in the middle of a sedimentary succession formed in jurassic basins which changed cyclically their depth because of the basement movement. Since the sequence is defined on chrono-stratigraphical basis, the inter-formation boundaries do not correspond, necessarily, to lithological changes. Thus, the actual thickness of the clay bed must also account for the lower 40-50 metres of the overlying Corallian Beds, equally constituted by clayey sediments. Then, the total thickness of the potential host rock is about 100 metres.

Major trends of groundwater flow through the sedimentary sequence are shown in Fig. 1. Groundwater movement through the Oxford Clay and

mudstone facies of the Corallian is predominantly vertical toward the Corallian aquifer. However, due to the very low hydraulic conductivity of the Oxford Clay ($\sim 3 \cdot 10^{-12}$ m/s), the rate and the volume of groundwater flow through it are extremely small. The estimated transit time from a central point in the mudstone sequence to the Corallian aquifer is about $5 \cdot 10^5$ a. In any way, no groundwater from the Oxford Clay could reach the surface at the Harwell site under the natural gradients presently prevailing.

Conversely, the major component of flow across the high permeability layers is approximately horizontal. The shallowest unconfined aquifer acts as the most important drainage system in the area. The geology of the Harwell region is shown in Fig. 2. A NNW-SSE cross section through the Harwell site is shown in Fig. 3, together with the groundwater flow pattern and recharge areas inferred from head measurements in several wells drilled in the region. Within the Corallian aquifer mixing occurs between groundwater flowing updip from SSE and water flowing from the recharge area. This is the reason for low groundwater heads and high mineral content within the Corallian aquifer west of Abingdon under the outcropping Kimmeridge clays. To the southeast of Abingdon an overflowing area is shown in Fig. 4. Artesian waters from the Corallian feed here the rivers merging eastwards into the Thames. In the vicinity of Abingdon the Corallian is important, sustaining a number of industrial abstractions where yields up to $3 \cdot 10^5$ m³/a are obtained, which make 12% of total formation contribution to groundwater supplies in the Harwell region. Hydraulic conductivity of the Corallian aquifer in the vicinity of the Harwell site is about $3 \cdot 10^{-7}$ m/s. This value multiplied by the local hydraulic gradient of $3.3 \cdot 10^{-3}$, gives a velocity of the water of approximately 10^{-9} m/s. Higher hydraulic gradients are found in the northeast region in the neighbourhood of the Thames valley, in the order of $2.2 \cdot 10^{-2}$.

3.2 Repository design

It is assumed that the repository lies in the middle of the mudstone-clay sequence (depth to the top 260 m).

The repository design foresees a set of parallel galleries with an overall thickness of 5 metres, accounting for 3.5 m for the gallery plus 1.5 m of lining and disturbed zone. Backfilling thickness is 1 m and it is made up of concrete.

3.3 Waste inventory

Considering the exploratory character of this study, no special effort was made to define the alpha-waste inventory on a more concrete basis, and we utilized the broad data which are currently available in the open literature (/8, 9 and 10/).

The waste inventory utilized for the present exercise is based on the following assumptions:

- electronuclear energy produced: 1000 GW(e)·Y, generated by 33 reactors, of the LWR type, operated for 33 years;
- total spent fuel reprocessed: 30.000 tons;
- the fuel reprocessing plant is considered as the only source of alpha-bearing waste. It is assumed that 360.000 tons of conditioned alpha waste (CAW) are generated, which contain 0.5% of the processed plutonium, in total 1.35×10^6 g of Pu embedded into a concrete matrix, at the average concentration of 3.75 g/t.

Table I shows the concentration (moles/kg of CAW) of the different nuclides, at a time $t = 40$ years after fuel reprocessing:

Pu 238	$2.941 \cdot 10^{-7}$	Th 229	$2.151 \cdot 10^{-15}$
Pu 239	$9.226 \cdot 10^{-6}$	Th 230	$7.094 \cdot 10^{-11}$
Pu 240	$3.771 \cdot 10^{-6}$	Th 232	$1.445 \cdot 10^{-11}$
Pu 241	$1.641 \cdot 10^{-5}$	Np 237	$1.380 \cdot 10^{-7}$
Pu 242	$5.922 \cdot 10^{-7}$	Ra 226	$1.361 \cdot 10^{-14}$
Pa 231	$2.119 \cdot 10^{-12}$	C 14	$1.753 \cdot 10^{-8}$
U 233	$6.349 \cdot 10^{-12}$	Tc 99	$4.633 \cdot 10^{-7}$
U 234	$6.530 \cdot 10^{-7}$	Cs 135	$1.118 \cdot 10^{-6}$
U 235	$2.777 \cdot 10^{-5}$	Sn 126	$3.757 \cdot 10^{-7}$
U 236	$1.185 \cdot 10^{-5}$	Zr 93	$1.687 \cdot 10^{-4}$

4. RELEASE SCENARIOS IDENTIFICATION

On the basis of the described hydrology and of the geographic-geomorphologic characteristics of the site, a number of possible release scenarios have been identified which are summarized in Fig. 5. The present analysis is limited to the assessment of consequences from the normal scenario of radionuclides release because of the limited information available at this stage.

4.1 Normal scenario

The general features of the present geological setting and hydrologic regime are assumed to hold in this scenario. Migration of radionuclides occurs by leaching of the waste form and by diffusion through the back-filling and by diffusion/advection of groundwater through the host formation. Eventually the contaminated solution reaches the overlying Corallian aquifer where it is tapped by an abstraction well and used for

consumption by the local community.

At present most water in the area is supplied by the shallow aquifer which yields large volumes of water contributing for almost 75% of total needs. The modelled scenario foresees abstraction of roughly $8 \cdot 10^5 \text{ m}^3/\text{a}$ of groundwater from boreholes drilled in the Corallian within the overflow area about 5 km from the site. Other abstraction areas are not considered in the assessment since, where contamination is likely to occur, either groundwater has a high salinity and cannot be exploited for consumption or there are shallow aquifers at easy reach. Contamination from the repository to the underlying aquifer (Great Oolite Group) should account for water migration through fractures. In fact, permeability tests in the laboratory yield values about 15 times lower than those measured in situ. There is insufficient information on the regional groundwater flow and it is difficult to imagine an emergence point for such an aquifer.

5. MODELLING

A special near-field/buffer model was built to simulate cement degradation effects. The biosphere model was simplified and reduced to a set of parameters converting a radionuclide concentration in the solution to a dose rate.

5.1 Concrete degradation and near-field diffusion

Both the waste matrix and the backfilling are made up of concrete and their continuing degradation allows for waste leaching and release. In the model, concrete is treated as a porous medium whose characteristics progressively deteriorate while maintaining a porous skeleton. Concrete degradation involves the release of Ca(OH)_2 , and the establishment of a very high pH, at which most of the radioelements are highly insoluble.

As long as the concrete is not completely dissolved, the high pH of the near field will limit the radionuclide release to a very low level. For this reason, the concrete lifetime is the critical parameter of the system.

The degradation process can be described by successive steps:

Phase 1: When cement is in contact with water, the tricalcium silicate $(\text{CaO})_3\text{SiO}_2$ forms a hydrated calcium silicate $\text{CaOSiO}_2 \cdot \text{H}_2\text{O}$. As a consequence, the pH in the surrounding increases up to a maximum equilibrium value of 12.5 which corresponds to the solubility limit of $\text{Ca}(\text{OH})_2$ (1.14 g/l as CaO at 25°C). The reaction proceeds at a constant pH up to the total degradation of $(\text{CaO})_3\text{SiO}_2$. The flux of $\text{Ca}(\text{OH})_2$ during this step is computed as

$$FI = S C_{cs} V \text{ (moles/a)}$$

where:

C_{cs} = $\text{Ca}(\text{OH})_2$ solubility (moles/m³) at pH = 12.5

V = interstitial water velocity (m/a) at the interface

S = effective concrete surface for leaching (m²).

During this step, flux, retention factors and solubilities stay constant until time T_c computed from

$$\int_0^{T_c} FI(t) dt = Q_c x_c / M_c$$

where:

x_c = concrete weight fraction of $\text{Ca}(\text{OH})_2$ released during tricalcium silicate hydration

Q_c = total concrete amount (waste + buffer, kg)

M_c = $\text{Ca}(\text{OH})_2$ molecular weight.

The radionuclides are divided into a precipitated fraction Q_1 (moles) and a fraction in solution at the solubility limit concentration C_{s1} (moles/m³).

Phase 2: Tricalcium silicate hydration is completed, pH is lowered to ~10.5. Solubilities of the various nuclides change to new values C_{cs1} and retentions change to new values R_{i1} . Flux of $\text{Ca}(\text{OH})_2$ from concrete now is:

$$FI_1 = S \cdot C_{cs1} \cdot V$$

where:

C_{cs1} = $\text{Ca}(\text{OH})_2$ solubility at pH = 10.5.

This step lasts until time T_{cl} computed as:

$$\int_{T_c}^{T_{cl}} FI_1(t) dt = Q_c x_{cl} / M_c$$

where:

x_{cl} = residual $\text{Ca}(\text{OH})_2$ fraction in concrete.

Phase 3: Concrete degradation is now complete giving a silica gel as final product. PH has dropped to the value typical of the original groundwater. Nuclide solubilities change to new values C_{si2} and retentions to R_{i2} .

The transport model for nuclide diffusion from the waste form to the host formation during the degradation phases is described by the following equations:

$$\frac{\partial C_i}{\partial t} = \frac{D}{R_i} \frac{\partial^2 C_i}{\partial x^2} \quad \text{dissolved fraction} \quad (1)$$

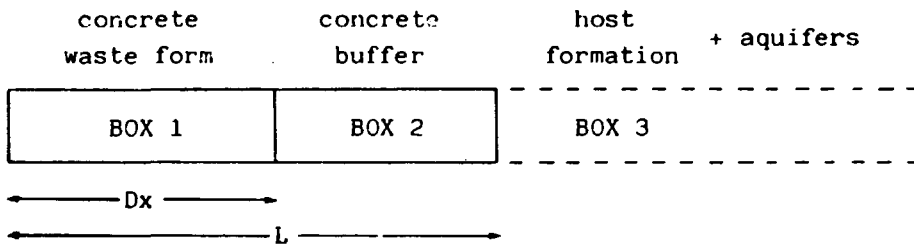
$$\frac{\partial Q_i}{\partial t} = S \frac{D}{R_i} \text{Dx} \left(\frac{\partial C_i}{\partial x} \right)_{x = \text{Dx}} \quad \text{precipitated fraction} \quad (2)$$

where:

Dx is the buffer thickness and

$$\begin{array}{ll}
 C_i(x,t) = C_{si} & t < T_c \\
 R_i(x,t) = R_i & t < T_c \\
 C_i(x,t) = C_{si1} & T_c < t < T_{cl} \\
 R_i(x,t) = R_{i1} & T_c < t < T_{cl} \\
 C_i(x,t) = C_{si2} & t > T_{cl} \\
 R_i(x,t) = R_{i2} & t > T_{cl}
 \end{array}$$

The described system may be represented by the following model



All precipitation-redissolution processes are assumed to take place in Box 1. The model describes processes occurring in both box 1 and 2 which represent the near field. The far field is described in box 3.

Boundary conditions are:

$$C_i(L,t) = 0 \text{ (infinite dilution at concrete/host formation interface),}$$

where L is the buffer thickness

$$C_i(x,t) = C_{si} \text{ for } x < Dx \text{ and } t < T_c$$

$$Q_i = Q_i^0 \text{ at } t=0; Q_i^0 = Q_i \text{ (inventory at } t=0) - C_{si} SDx \text{ where } Q_i(t) \text{ is}$$

the amount precipitated in box 1.

This model assumes that the rate of degradation is controlled by the rate of diffusion of Ca(OH)_2 away from the concrete, i.e. hydration kinetics are considered fast. At high water fluxes this might be unrealistic. The fraction X_c of CaO released during tricalcium silicate hydration needs to be estimated. Experimental data of nuclide sorption on crushed cement (at high pH) are available, but their variation with dropping pH must be estimated. Retention should depend strongly also on physical degradation of concrete, so it should vary with the position along the migration direction as well as with time. Conservative assump-

tions should be made in order to keep them constant along the column for each of the three time transients.

For Ca(OH)_2 solubility, laboratory data are used /11/.

5.2 Far-field model

The near-field model provides the source term for the far-field model which simulates radionuclide migration/sorption processes in the mudstone-clay sequence and in the Corallian aquifer (box 3). The two geological units are modelled separately and called in succession by the far-field routine. Their hydraulic parameters and sorption characteristics are basically different and this makes diffusion processes to prevail in the host formation and advection/mechanical dispersion phenomena to prevail in the aquifer. Sorption data of nuclides in mudstone have been taken equal to those previously used for a typical clay formation /5/. For the aquifer they have been taken conservatively one order of magnitude smaller.

5.3 Biosphere

The rates of the various radionuclides resulting from the far-field are then fed into the biosphere model. The geosphere/biosphere interface is a water abstraction point (a well or a river) at a given distance from the repository and with a given flow rate. The output from the biosphere is a dose rate (Sv/a). In this exercise the biosphere model has been drastically simplified because the quality of the biosphere data in this context does not justify the simulation of the biosphere transport by a compartment model. In addition, the use of a large number of parameter distributions for biosphere transfer coefficients would increase the total uncertainty of the calculated dose rates hampering the subsequent sensitivity analysis. Therefore, a lumped parameter approach was used. Since the biosphere model is a linear one, it is possible to substitute

the biosphere subroutine by distribution functions quantifying the conversion from concentration in the well water to an annual dose. It has been found by comparison with observed data that Weibull distribution functions perform properly for this purpose. In this way a reduction of the number of sampled parameters in the system model is obtained and less computer time for the calculation is used.

6. RESULTS

The input data set for the present assessment exercise consists of a set of 74 probability distributions (log normal, log uniform, uniform and Weibull) representing the geochemical and transfer coefficients of the 10 decay chains considered plus the hydrogeological parameters of the site.

100 runs were performed and the analysis gives dose rate distributions up to 10^6 years after repository closure.

Fig. 6 and Tables II and III show the distribution of the maximum individual dose rate due to the ingestion pathway considered. It can be observed that the uncertainty range of the results is spread over several orders of magnitude; however only a very small fraction of the results (less than 3%) yields dose rates larger than 10^{-5} Sv/a.

The maximum dose obtained (0.45×10^{-2} Sv/a) is of the same order of magnitude of the natural background level.

High doses are entirely dominated by Th 230 mainly because of the relative mobility of its parent U 234 and its high radiotoxicity. Several other nuclides contribute to the overall dose, and a map of their distribution within the maximum doses histogram is shown in Table I.

A picture of dose rate distributions at 10^5 years and at 10^6 years is given in Fig. 7 and Fig. 8.

In Fig. 9 the mean values of the total dose rates are plotted as a function of time. The curve shows an initial period (about 10,000 years) of

very low doses and then a steep increase up to 100.000 years.

Afterwards mean values fluctuate around 10^{-6} to 10^{-5} Sv/a.

The same figure shows also the plot of the 95th percentile as a function of time which indicates the dose value exceeded by only 5% of the runs, i.e. by 5 runs in our case. It is very significant that this curve rests 3 to 4 orders of magnitude below the mean curve around 100.000- 200.000 years. This means that the high mean doses are due to very few runs and are strongly emphasized by the logarithmic scale of the plot. It may be observed that for time periods shorter than 250.000 years after repository closure, 95% of the simulations result in a very low dose reaching at most 0.1 micro Sieverts/a.

A double check on the radionuclides responsible for high doses was performed by running the code again 100 times with only the three major input chains: Pu 239, Pu 238 and Am 241 chains.

The results are of course identical for the highest doses runs while in the other runs the lack of contribute from the other nuclides is evident (Fig. 10).

The plots of dose contribution of the 5 most important nuclides versus time are also equal (Fig. 11 and Fig. 12).

A difference can be observed in the mean and 95th percentile plots (Fig. 9 and Fig. 13), where, in the 3 chains case, there is a period of about 100.000 years of very low doses probably due to the presence of only long half life nuclides.

7. SENSITIVITY ANALYSIS

Parameters which strongly affect model results are identified by comparing the input data values associated to the highest doses and the probability distributions assigned (Smirnov test /2/).

The analysis was performed on both input sets (10 chains and 3 chains) to check its significance in assessing the importance of the parameters

in a large and in a small input data set.

The results show that several parameters are responsible in governing the model output and the most important are: water velocity in the aquifer, flowrate (VA, FLOWR), (Figg. 14 and 15), pathlength in the mudstone (XPM) and in the aquifer (XPA) and retention properties of some nuclides in the geosphere. By comparing the plots from the two different analysis it has been observed that even though results are very similar, some parameters, such as velocity in the aquifer, seem to be more important in the 10 chains case while flowrate and pathlengths are more important in the 3 chains case. This is probably due to the fact that in the latter case parameters that affect Thorium behaviour are more evident. The important role of these variables is confirmed by the Spearman test which gives the following coefficients:

Variable	rho (10 chains)	rho (3 chains)
VA	0.61	0.49
K1(U)	- 0.34	- 0.31
FLOWR	- 0.30	- 0.21
XPA	- 0.17	- 0.17
DIFFCO	0.13	0.21
XPM	- 0.04	- 0.18

This analysis indicates the general effect of parameters on the resulting dose, while the Smirnov test is related only to the highest doses runs. That is the reason why the two analysis methods may point out different variables.

Unfortunately the uncertainty linked to some of these parameters cannot be eliminated because they are intrinsically unpredictable; for other parameters a better definition might be achieved by progress in research work.

Despite the uncertainty of conditioning matrix parameters, it is interesting to note that none of them has been highlighted by the sensitivity analysis.

8. CONCLUSIONS

The exercise shows that the model and methodology can be applied in assessing the safety of an alpha waste deposit. It is obvious that in evaluating the performance of a real site, better data and a more sophisticated biosphere model are needed.

The analysis of the normal evolution scenario, with well water withdrawal and consumption, indicates that output doses to an individual in the critical group are acceptable. Probabilistic scenarios should also be modelled and consequences evaluated.

Both the cases analyzed show that Th 230 is a critical radionuclide but in general retention properties and solubilities of transuranics in different media and at different pHs must be defined with a better accuracy. The fact that Np 237 does not appear among the risk-governing radionuclides, as it occurred in previous assessments /5/, is due to the over-conservative estimates of Np dose factor in the past. The new figures defined by ICRP make this radionuclide less important.

The indication given by the former assessment /5/ on vitrified waste disposal suggested that the role of alpha-waste is undoubtedly significant; moreover the information concerning leaching properties of conditioned alpha-waste was very scarce, so that the release rate assessed for this material were affected by a very large uncertainty. A more thorough knowledge of this conditioning ways and properties was hoped.

The present study confirmed the importance of alpha-waste in risk assessments . Furthermore it points out the major role played by the host formation and the surrounding geology with respect to the leaching characteristics of the conditioning matrix: the source term generally is not critical, the long term doses being strongly dependent on geosphere features.

This study confirms the results of previous experiences which are very encouraging in this context, given the difficulty in characterizing near-field alpha-waste form behaviour.

REFERENCES

- /1/ CADELLI N., COTTONE G., BERTOZZI G., GIRARDI F.;
"PAGIS, Performance Assessment of Geological Isolation Systems.
Summary report of phase 1"; Report EUR 9220 EN (1984).
- /2/ BERTOZZI G., HILL M.D., LEVI G., STORCK R.;
"Long-term risk assessment of geological disposal: methodology and
computer codes"; Proc. of the 2nd European Community Conf. on Rad.
Waste Management and Disposal; Luxembourg, 22-26 april 1985; pp.
639-651, report EUR 10163, Cambridge University Press, (1986).
- /3/ ICRP Publication 46, Annals of the ICRP, 15, 4 (1985).
- /4/ SALTELLI A., BERTOZZI G., STANNERS D.A.;
LISA, A Code for Safety Assessment in Nuclear Waste Disposal, Pro-
gram Description and User Guide; Report EUR 9306 EN (1984).
- /5/ BERTOZZI G., D'ALESSANDRO M., SALTELLI A.;
Waste Disposal into a Plastic Clay Formation, Risk Analysis for
Probabilistic Scenarios, EUR 9641 EN (1984).
- /6/ ALEXANDER J.;
The Groundwater Regime of the Harwell Region; Fluid Processes
Unit-Institute of Geological Sciences FLPV 83-10 (1983).
- /7/ ALEXANDER J., HOLMES O.C.;
The Local Groundwater Regime at the Harwell Research Site; Fluid
Processes Unit-Institute of Geological Science FLPV 83-1 (1983).
- /8/ NAGRA, Project Gewähr (1985), NGB-85-09.
- /9/ SIMON R., Proposal for Waste Types and Forms to be included in PACOMA
(1986), CEC Bruxelles, personal communication.
- /10/ AECL, Report on Risk Assessment exercise
- /11/ LEA F.M., "The Chemistry of Cement and Concrete"; 3rd Edit.; Edward
Arnold Publisher (1980).
- /12/ SCK/CEN, Sensitivity and Uncertainty Analysis for the Normal Evolu-
tion Scenario; Reference Repository in the Boom Clay at Mol. (1987).
- /13/ CONOVER W.J.;
"Practical Nonparametric Statistics"; 2nd Edition, John
Wiley & Sons, (1980).

ACKNOWLEDGMENTS

This work was made possible by the kind assistance provided by the BGS (British Geological Survey) of Nottingham, U.K., who helped in gathering all the available information and data.

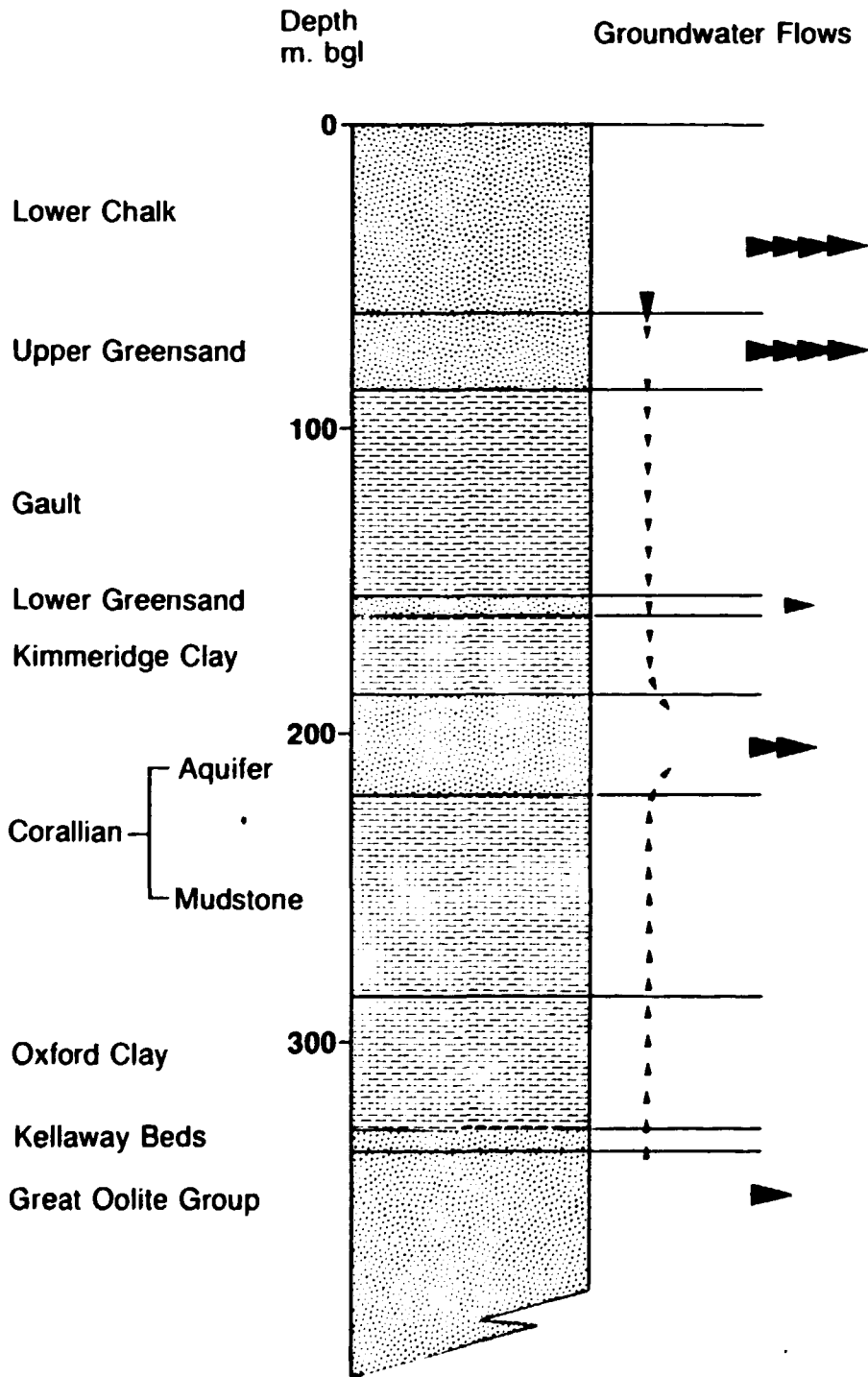


Fig. 1 Groundwater flow pattern under the Harwell Research Site
(From J. Alexander and D.C. Holmes, 1983)

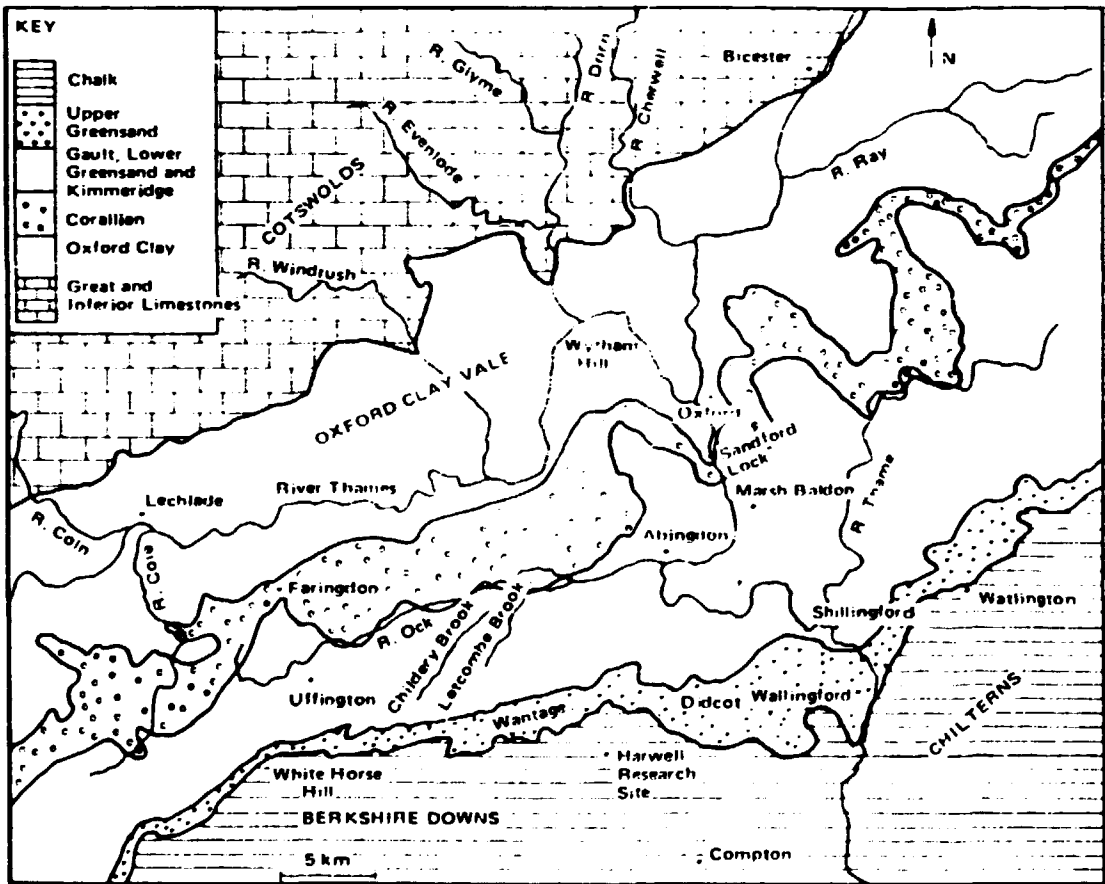


Fig. 2 Geology of the Harwell Region
 (From J. Alexander, 1983)

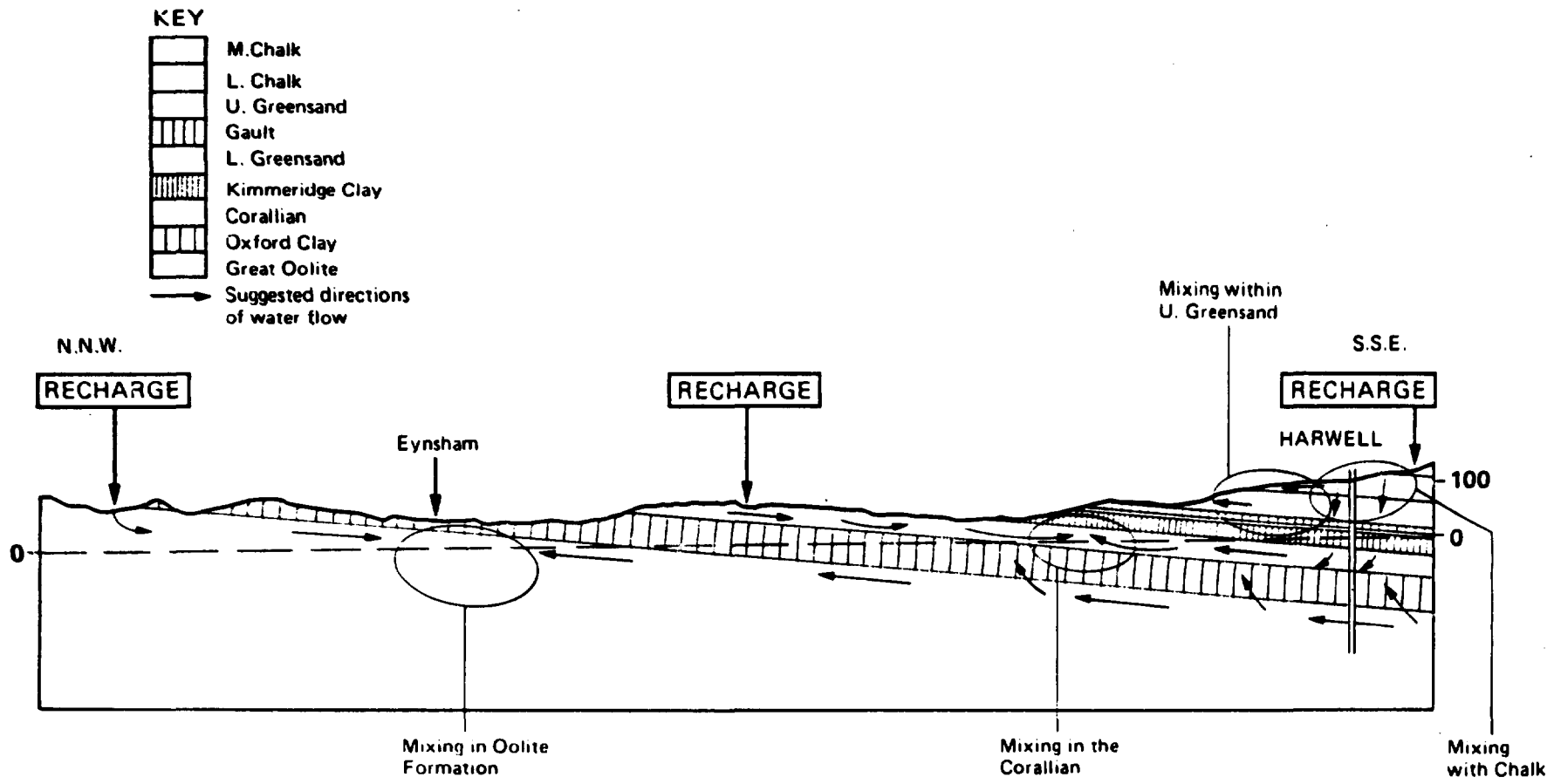


Fig. 3 Groundwater movement in the Harwell region and mixing patterns
 (From J. Alexander, 1983)

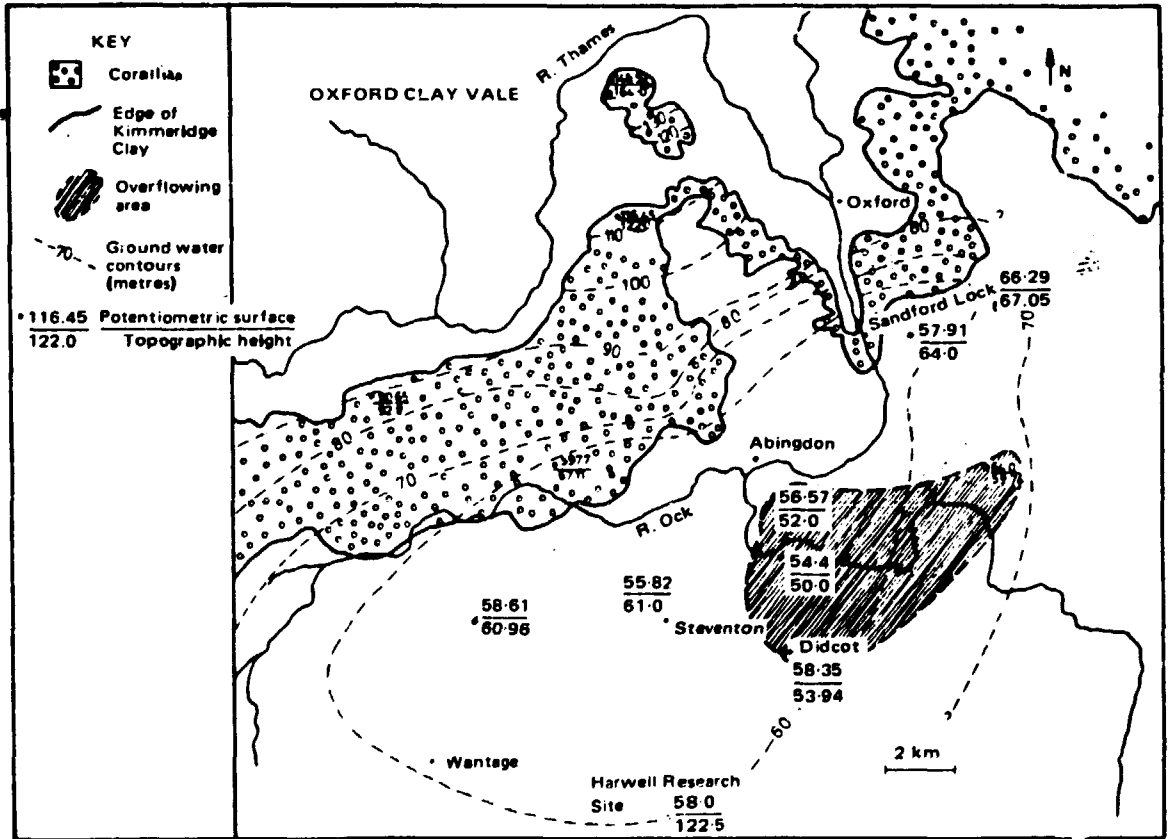


Fig. 4 Groundwater contours: Corallian
 (From J. Alexander, 1983)

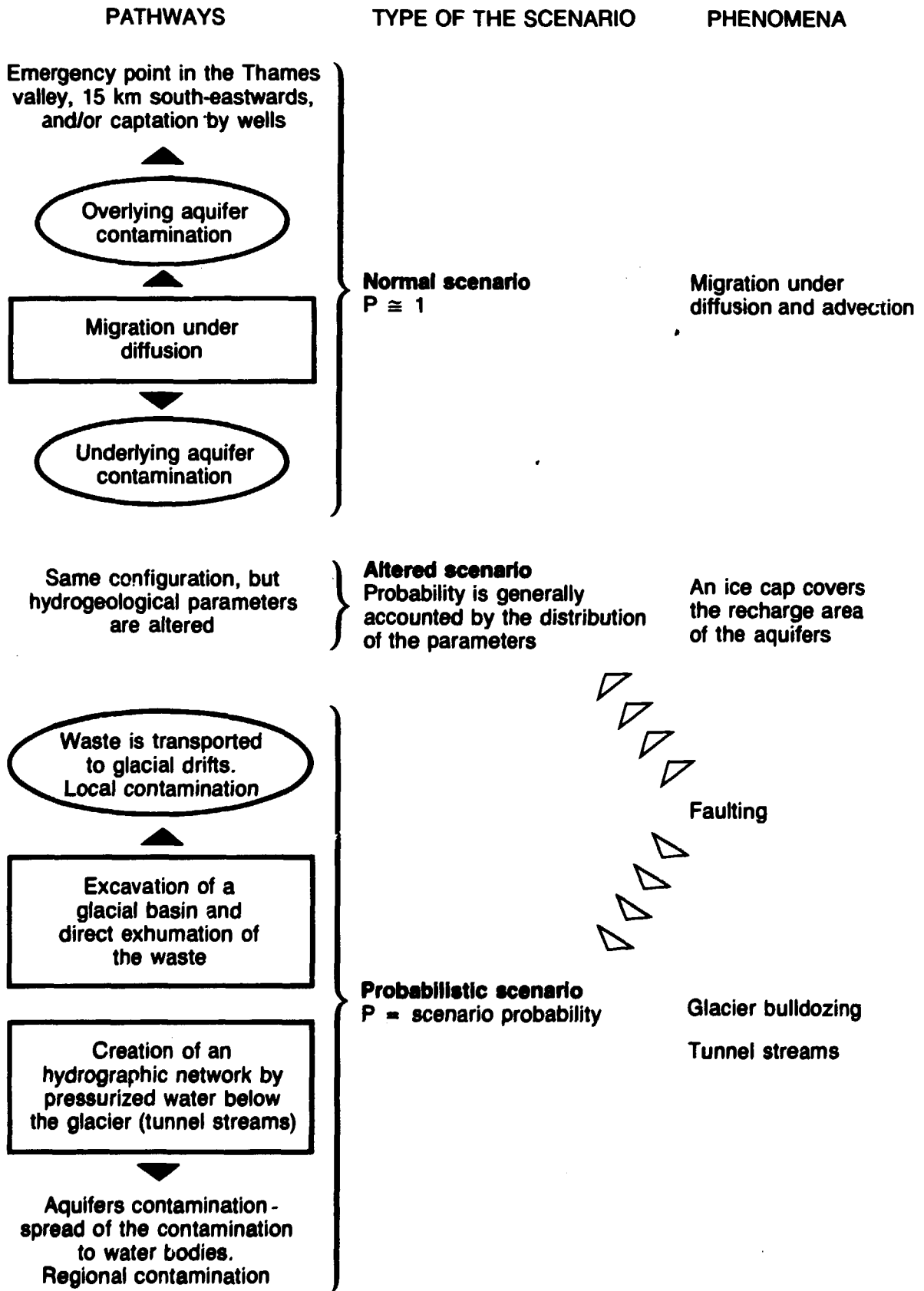


Fig. 5

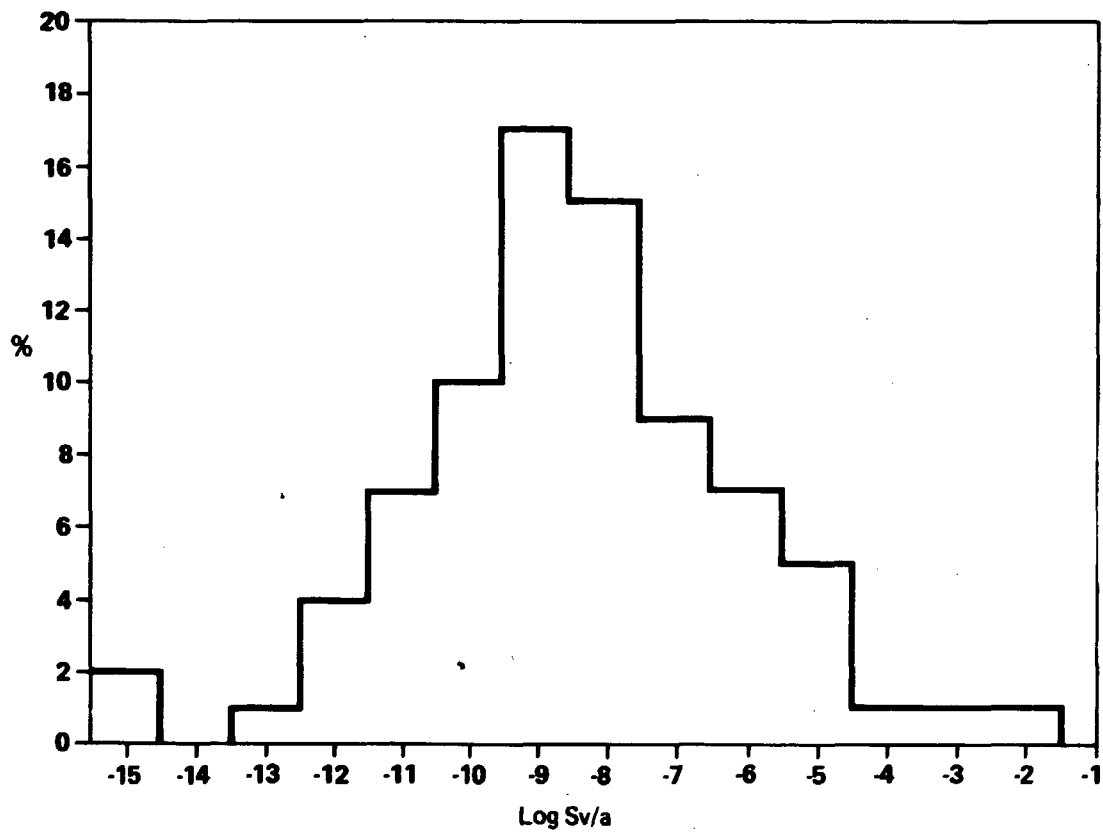


Fig. 6 Maximum individual dose rates (10 chains)

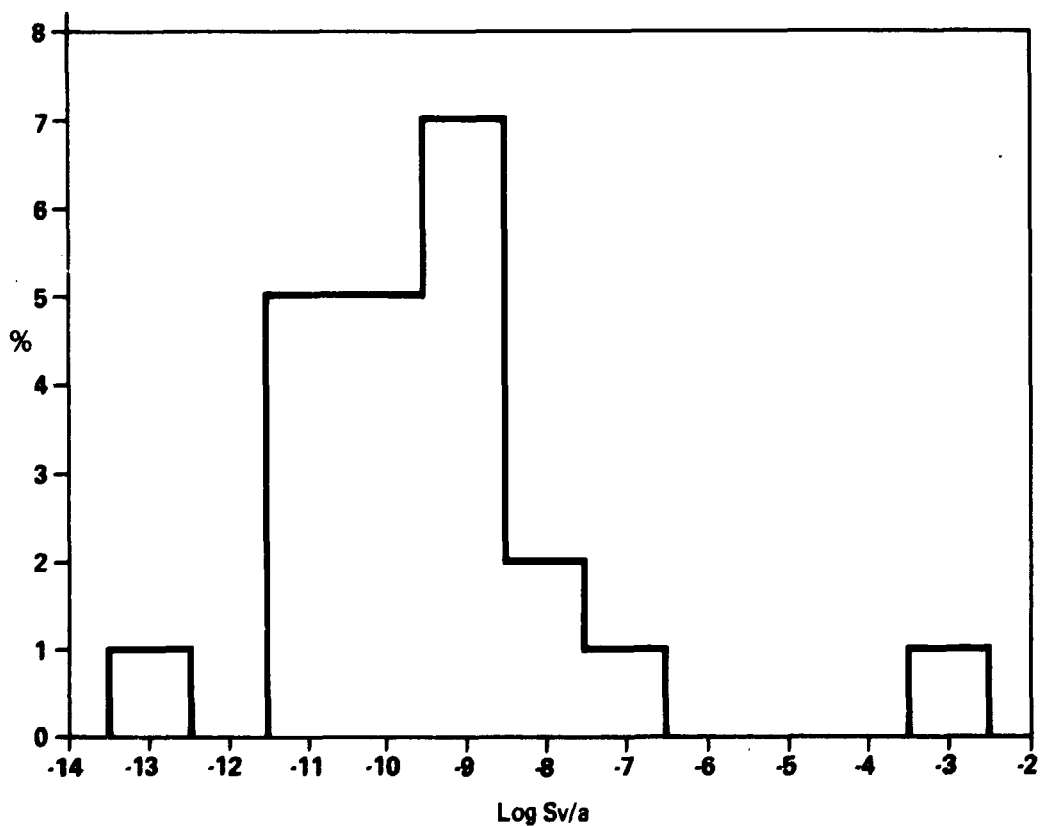


Fig. 7 Doses at 10⁵ years (10 chains)

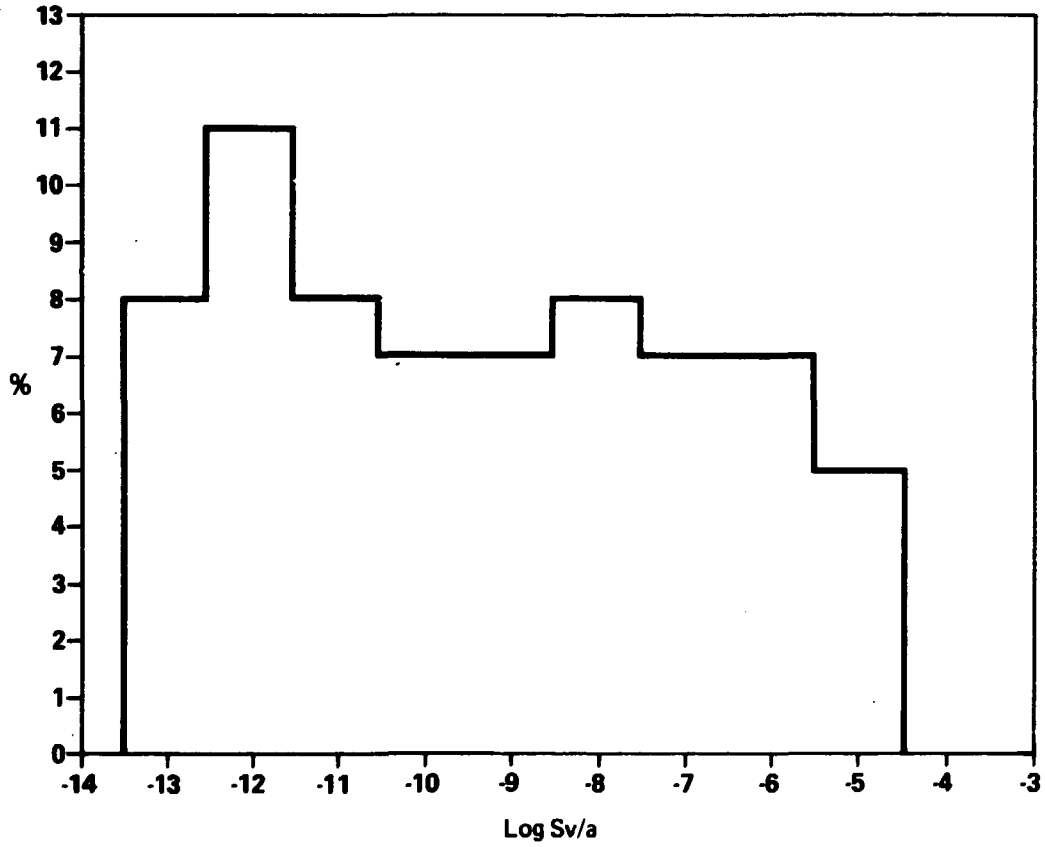


Fig. 8 Doses at 10^6 years (10 chains)

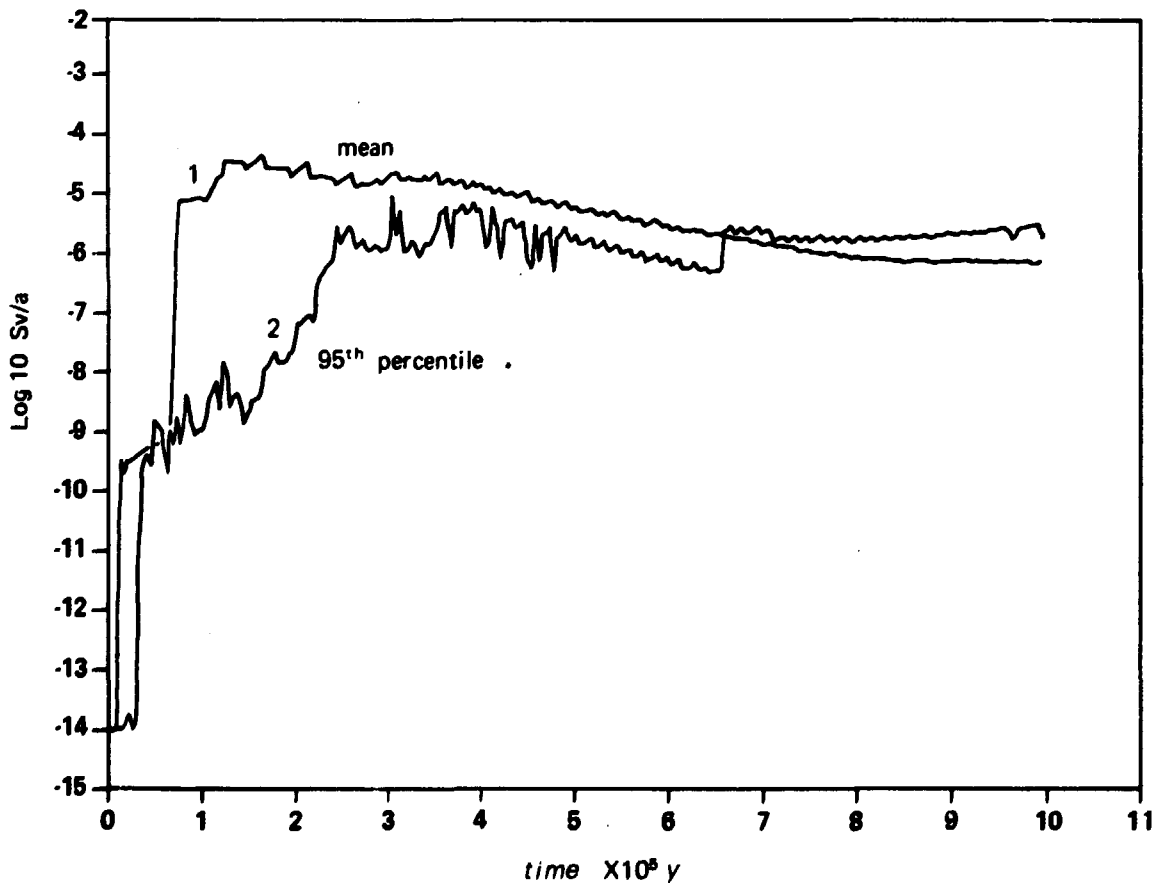


Fig. 9 (10 chains)
Dose rate mean values

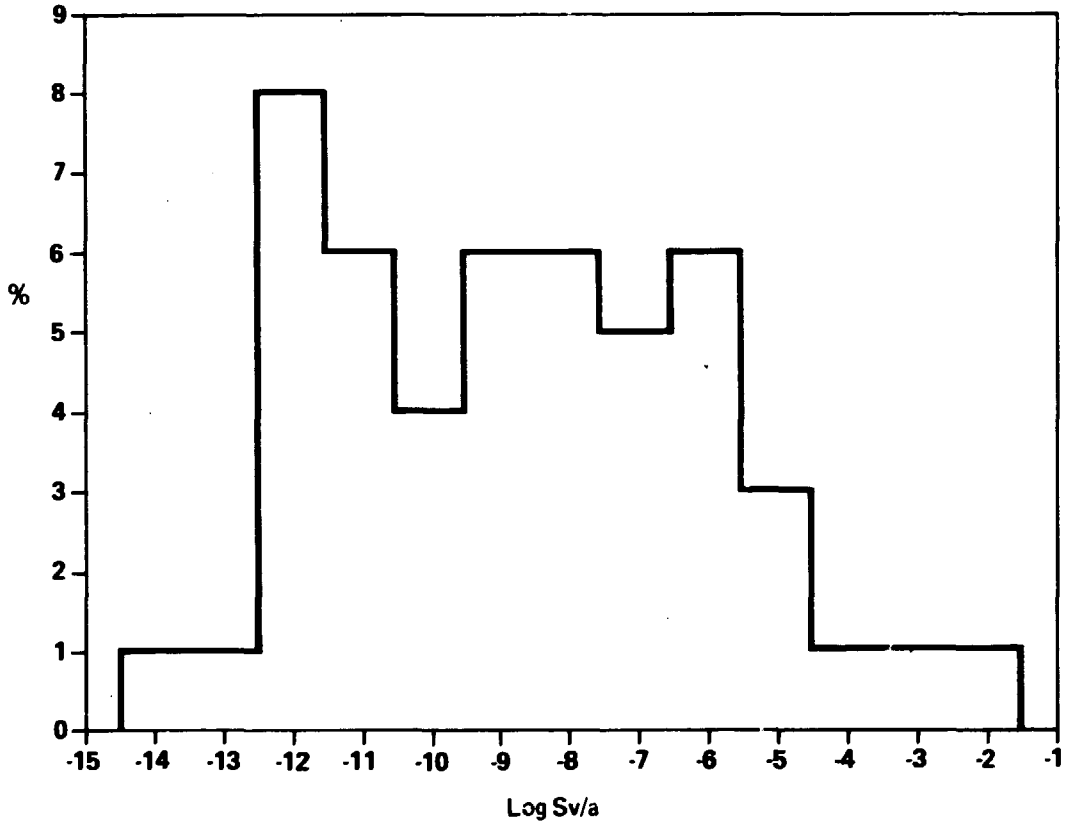


Fig. 10 Maximum individual dose rates (3 chains)

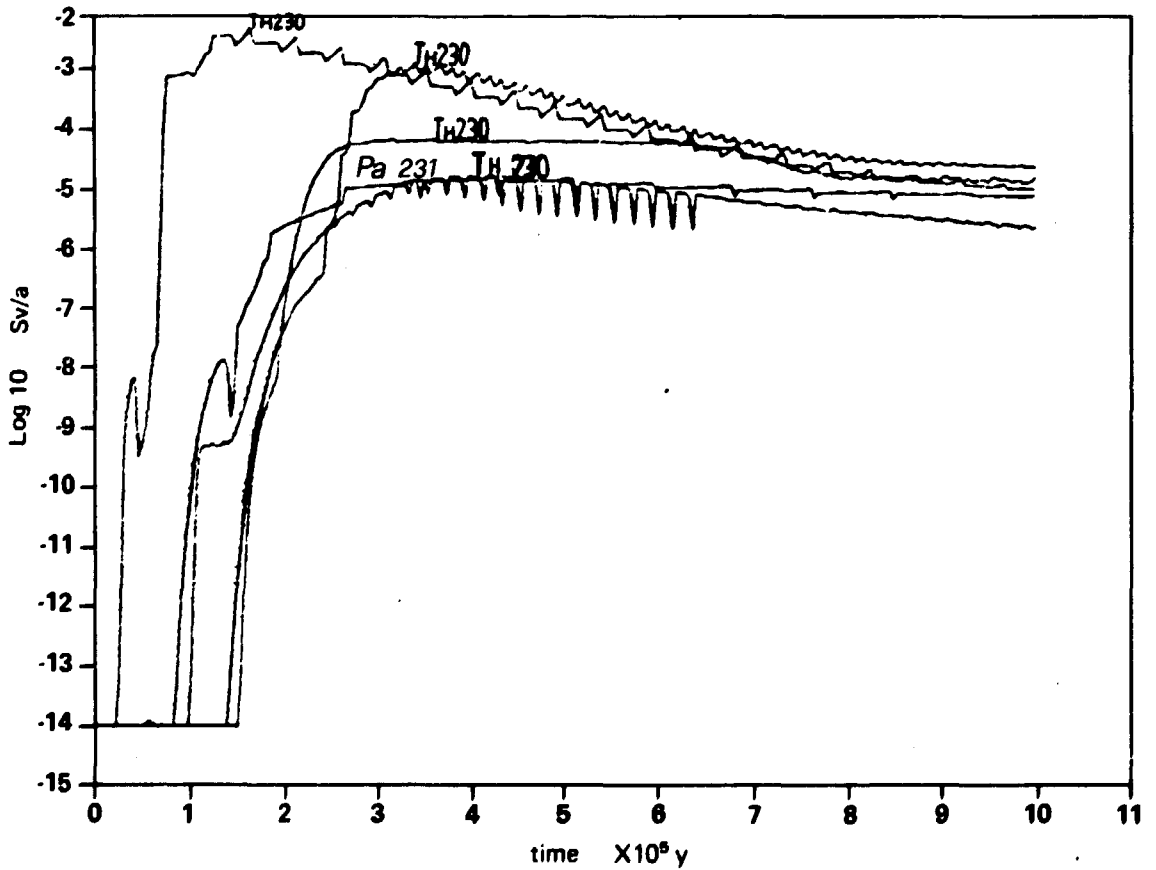


Fig. 11 (10 chains). Dose contribution of the most important nuclides versus time

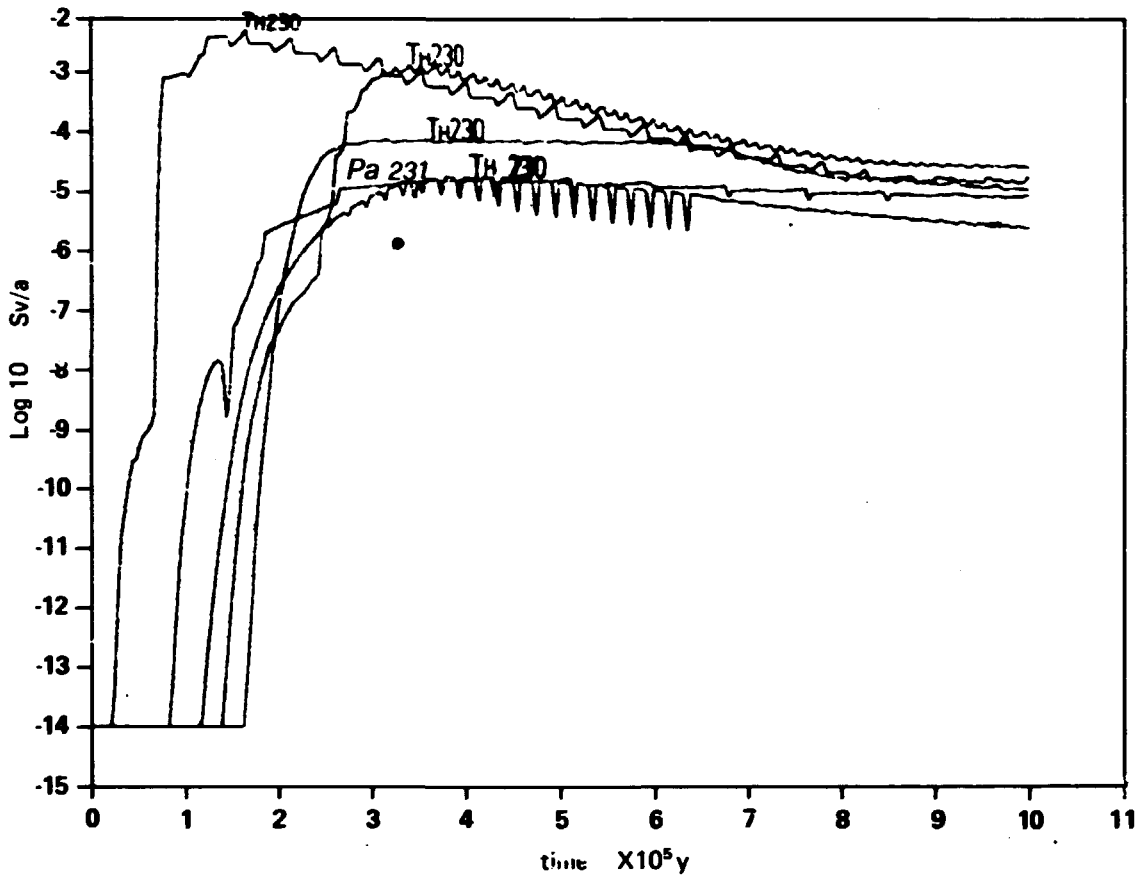


Fig. 12 (3 chains) — Dose contribution of the most important nuclides

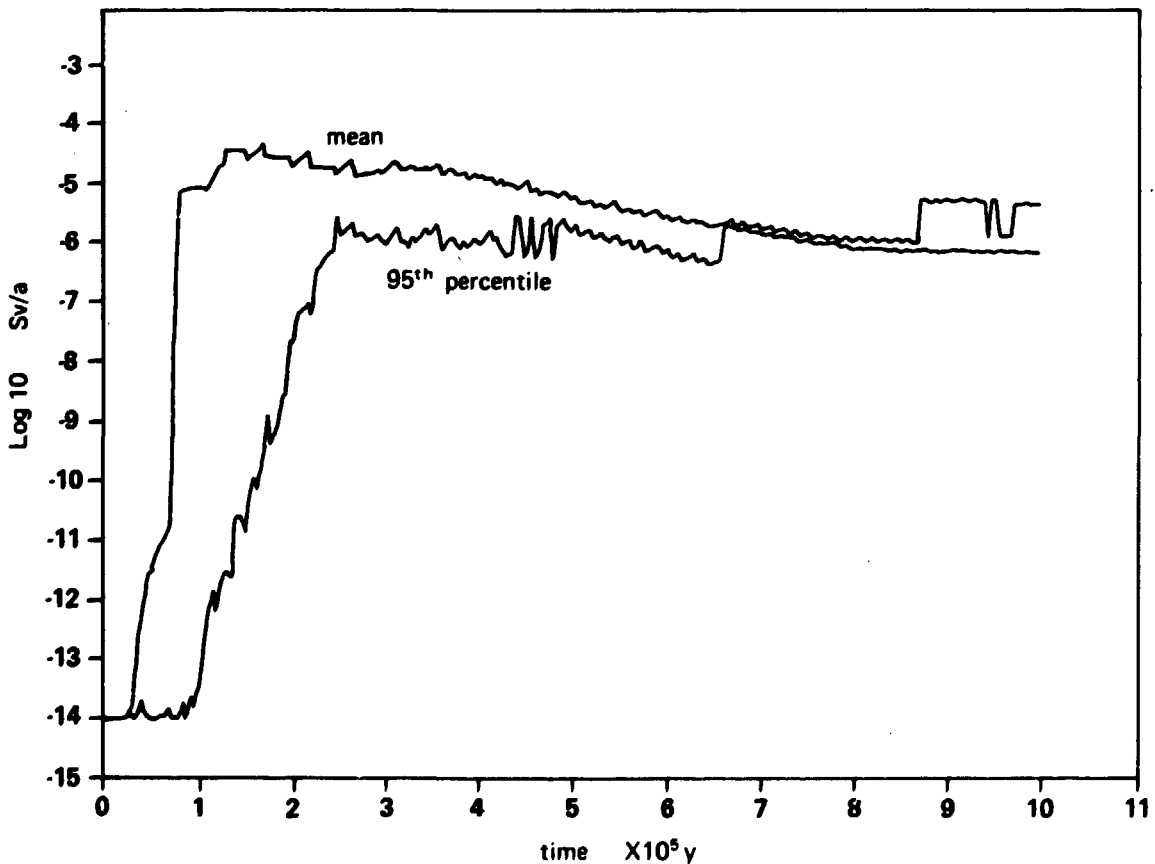


Fig. 13 (3 chains) — Dose rate mean values

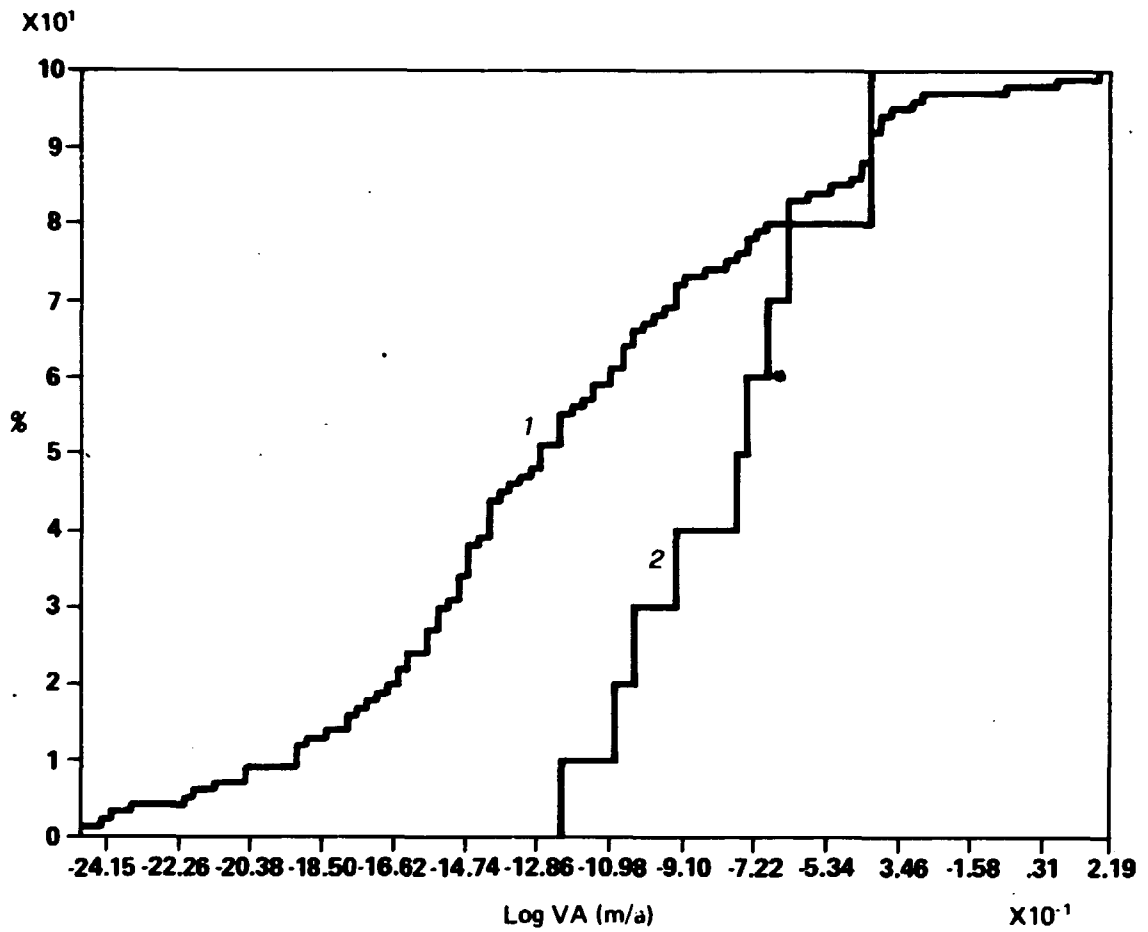


Fig. 14 (10 chains) curve 1 : cumulative distribution over 100 runs
 curve 2 : " " for the 10 highest doses runs

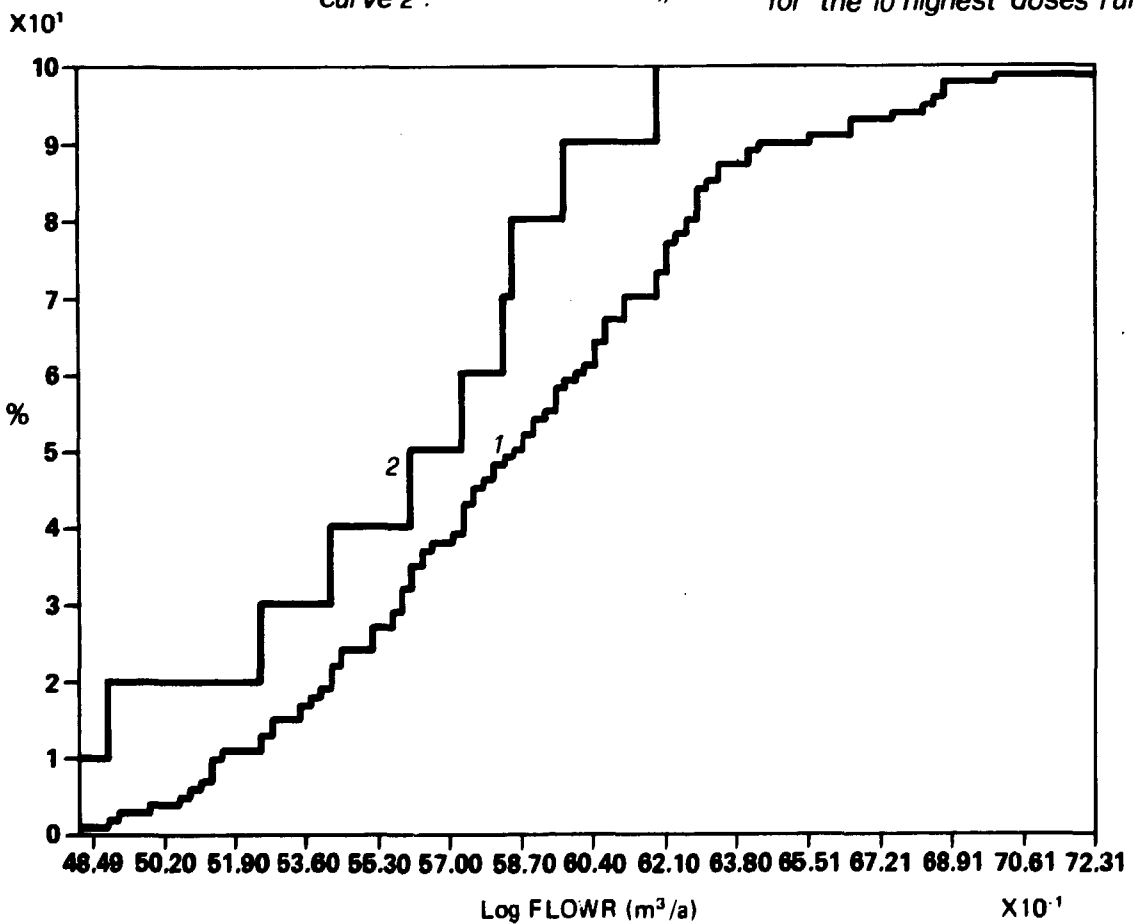


Fig. 15 (10 chains) curve 1 : cumulative distribution over 100 runs
 curve 2 : " " for the 10 highest doses runs

**Edito dall'ENEA, Direzione Centrale Relazioni
Viale Regina Margherita, 125 - Roma
Finito di stampare nel mese di dicembre 1987
Fotoripr. e Stampa «Arti Grafiche S. Marcello»
Viale Regina Margherita, 176 - 00198 Roma**